

Detection of ventricular thrombi via electron density imaging in non-contrast spectral computed tomography performed to exclude pneumonia: a case report

Junji Mochizuki ^{1*}, Takeshi Nakaura ², Katsushi Hashimoto³, and Yoshiki Hata ³

¹Department of Radiology, Minamino Cardiovascular Hospital, 1-25-1 Hyoue, Hachioji, Tokyo 192-0918, Japan; ²Department of Diagnostic Radiology, Graduate School of Medical Sciences, Kumamoto University, Kumamoto, Japan; and ³Department of Cardiology, Minamino Cardiovascular Hospital, Hachioji, Japan

Received 7 December 2021; first decision 14 January 2022; accepted 1 April 2022; online publish-ahead-of-print 5 April 2022

Case description

A 44-year-old man presented with emergent dyspnoea and lower extremity oedema. He had no other medical history and no risk factors for heart disease. The referring physician suspected bronchial asthma because of persistent cough, and salmeterol xinafoate and fluticasone propionate had been ineffective. Radiography showed pleural effusion, cardiomegaly, and pulmonary congestion, but pneumonia could not be excluded. Blood tests showed high levels of D-dimer (6.25 µg/mL) and N-terminal pro-B-type natriuretic peptide (5830 pg/mL), suggesting heart failure and aortic dissection,¹ the C-reactive protein level was normal (0.32 mg/L). Because the patient exhibited persistent cough, chest computed tomography (CT) with spectral CT was performed to exclude pneumonia prior to echocardiography. This case occurred during the coronavirus disease 2019 epidemic; the D-dimer level was high, and thrombosis was possible.² CT was prioritized because the cough and breathlessness symptoms hindered a long examination. Cardiac magnetic resonance imaging (MRI) was omitted because the patient struggled to maintain a supine position. Although non-contrast CT showed right lung pleural effusion, the findings enabled exclusion of pneumonia. Electron density imaging (EDI) is a spectral imaging method that measures electron density,³ whereas conventional CT does not. Conventional CT showed no hyperintense regions (*Figure 1A and B*), and EDI revealed incidental findings of hyperintense regions in both ventricles (*Figure 1C and D*; [Supplementary material online, Videos 1 and 2](#)). Transthoracic echocardiography revealed severe diffuse biventricular

hypokinesia (*Figure 1E and F*). These areas corresponded to thrombi on EDI, confirming the diagnosis of heart failure. To our knowledge, ventricular thrombi have not been identified on non-contrast spectral CT EDI. Non-contrast CT EDI may facilitate diagnosis when MRI and echocardiography are difficult to perform.

Lead author biography



Junji Mochizuki is a radiologic technologist at Minamino Cardiovascular Hospital. He got his master's degree from the International University of Health and Welfare. He has an interest in advanced cardiac CT imaging using spectral CT.

Supplementary material

[Supplementary material](#) is available at *European Heart Journal—Case Reports* online.

Acknowledgements

We thank Angela Morben, DVM, ELS, and Ryan Chastain-Gross, PhD, from Edanz, for editing a draft of this manuscript.

* Corresponding author. Tel: +81 42 637 8101, Fax: +81 42 637 8108, Email: mochizuki.j@minaminohc.jp

Handling Editor: Massimo Mapelli

Peer-reviewers: Annagrazia Cecere, Suzan Hatipoglu and Christoph Jensen

© The Author(s) 2022. Published by Oxford University Press on behalf of European Society of Cardiology.

This is an Open Access article distributed under the terms of the Creative Commons Attribution-NonCommercial License (<https://creativecommons.org/licenses/by-nc/4.0/>), which permits non-commercial re-use, distribution, and reproduction in any medium, provided the original work is properly cited. For commercial re-use, please contact journals.permissions@oup.com

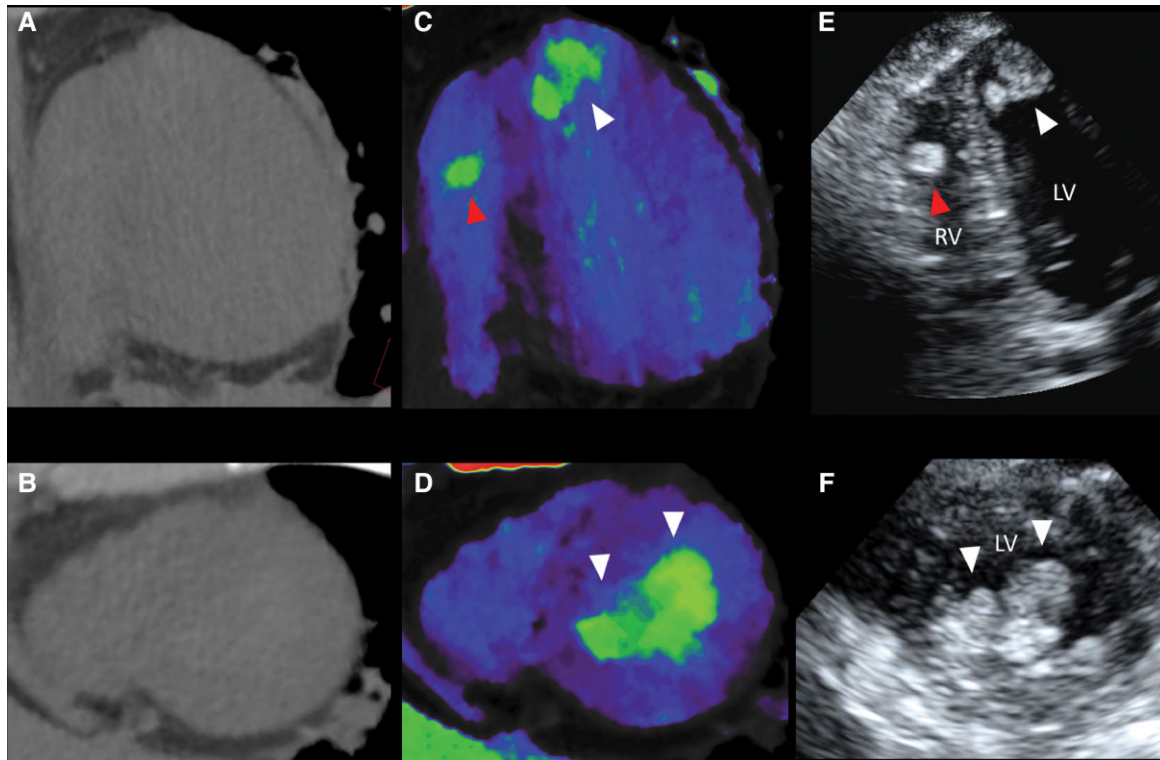


Figure 1 (A and B): Conventional 120 kVp computed tomography apical view (A) and short axis (B). (C and D): Fusion of conventional (120 kVp) and electron density computed tomography images of the apical view (C) and short axis (D). A 27.3 mm × 20.7 mm × 15.4 mm hyperintense region (Δ) is visible in the left ventricle; a 12.8 mm × 8.0 mm × 7.0 mm hyperintense region (▲) is visible in the right ventricle. The electron density values were 104.8% relative to the electron density of water (EDW) in the left ventricular cavity, 105.9% EDW in the left ventricular hyperintense region, 104.8% EDW in the right ventricular cavity, and 105.4% EDW in the right ventricular hyperintense region. The computed tomography numbers of the conventional images were 44.5 Hounsfield units (HU) in the left ventricular cavity, 58.0 HU in the left ventricular hyperintense region, 46.6 HU in the right ventricular cavity, and 52.3 HU in the right ventricular hyperintense region; these computed tomography numbers did not obviously differ among regions. (E and F): Transthoracic echocardiography findings in the apical view (E) and short axis (F). Diffuse severe wall hypokinesia was present in both left and right ventricles (left ventricular ejection fraction, 25%). A thrombus was evident in the area corresponding to the hyperintense region on the electron density image of the left and right ventricles.

Consent: The authors confirm that written consent for submission and publication of this case report, including images and associated text, has been obtained from the patient in accordance with COPE guidelines.

Conflicts of interest: none declared.

Funding: This research did not receive any specific grant from funding agencies in the public, commercial, or not-for-profit sectors.

References

1. Sbarouni E, Georgiadou P, Marathias A, Geroulanos S, Kremastinos DT. D-dimer and BNP levels in acute aortic dissection. *Int J Cardiol* 2007;**122**:170–172.
2. Gómez-Mesa JE, Galindo-Coral S, Montes MC, Muñoz Martin AJ. Thrombosis and coagulopathy in COVID-19. *Curr Probl Cardiol* 2021;**46**:100742.
3. Hua CH, Shapira N, Merchant TE, Klahr P, Yagil Y. Accuracy of electron density, effective atomic number, and iodine concentration determination with a dual-layer dual-energy computed tomography system. *Med Phys* 2018;**45**: 2486–2497.